Neurobiology of Disease

Dissociated Representation of Binaural Cues in Single-Sided Deafness: Implications for Cochlear Implantation

Peter Hubka,[1*] Leonard Schmidt,[1*] Jochen Tillein,[1,2,3] Peter Baumhoff,[1] Wiebke Konerding,[1] Rüdiger Land,[1] Mika Sato,[1] and Andrej Kral[1,4]

[1]Department of Experimental Otology, Institute of AudioNeuroTechnology, Clinics of Otolaryngology, Hannover Medical School, Hannover D-30625, Germany, [2]Clinics of Otolaryngology, School of Medicine, J.W. Goethe University, Frankfurt am Main D-60590, Germany, [3]MedEl GmbH, Starnberg 82319, Germany, and [4]Australian Hearing Hub, School of Medicine and Health Sciences, Macquarie University, Sydney, New South Wales 2109, Australia

Congenital single-sided deafness (SSD) leads to an aural preference syndrome that is characterized by overrepresentation of the hearing ear in the auditory system. Cochlear implantation (CI) of the deaf ear is an effective treatment for SSD. However, the newly introduced auditory input in congenital SSD often does not reach expectations in late-implanted CI recipients with respect to binaural hearing and speech perception. In a previous study, a reduction of the interaural time difference (ITD) sensitivity has been shown in unilaterally congenitally deaf cats (uCDCs). In the present study, we focused on the interaural level difference (ILD) processing in the primary auditory cortex. The uCDC group was compared with hearing cats (HCs) and bilaterally congenitally deaf cats (CDCs). The ILD representation was reorganized, replacing the preference for the contralateral ear with a preference for the hearing ear, regardless of the cortical hemisphere. In accordance with the previous study, uCDCs were less sensitive to interaural time differences than HCs, resulting in unmodulated ITD responses, thus lacking directional information. Such incongruent ITDs and ILDs cannot be integrated for binaural sound source localization. In normal hearing, the predominant effect of each ear is excitation of the auditory cortex in the contralateral cortical hemisphere and inhibition in the ipsilateral hemisphere. In SSD, however, auditory pathways reorganized such that the hearing ear produced greater excitation in both cortical hemispheres and the deaf ear produced weaker excitation and preserved inhibition in both cortical hemispheres.

Key words: **binaural sensitivity; cochlear implants; critical period; interaural level differences; unilateral deafness**

Significance Statement

Congenital single-sided deafness is a clinically relevant form of hearing loss. We studied this phenomenon in a unique animal model with congenital deafness in one ear and normal hearing in the other ear with electrical stimulation in both ears. Differential effects of single-sided deafness on interaural time and level difference sensitivity were observed, consistent with the aural preference syndrome. The influence of the previously hearing ear became dominant, and the deaf ear was mildly suppressive in the majority of units in both hemispheres, resulting in an inconsistent representation of binaural cues. These changes in neuronal representation of the two ears explain why late restoration with cochlear implants in single-sided deafness often results in insufficient benefits for the previously deaf ear.

Received Sept. 2, 2023; revised April 26, 2024; accepted April 26, 2024.

Author contributions: A.K. designed research; P.H., J.T., P.B., W.K., R.L., M.S., and A.K. performed research; P.H., L.S., and A.K. analyzed data.

The work was supported by the Deutsche Forschungsgemeinschaft (Exc 2271 and Kr 3370) and MedEl Comp., Innsbruck, Austria (provided the cochlear implants and supported J.T.). We thank Daniela Kühne for excellent her technical assistance. English-language support was provided by stels-ol.de. We thank the anonymous reviewers for their excellent suggestions that helped improve the manuscript.

*P.H. and L.S. contributed equally to this work.

The authors declare no competing financial interests.

Correspondence should be addressed to Andrej Kral at kral.andrej@mh-hannover.de or Peter Hubka at peter.hubka.1@gmail.com.

https://doi.org/10.1523/JNEUROSCI.1653-23.2024

Introduction

The brain must developmentally integrate the input from two cochleae. Asymmetric hearing during development interferes with this process (Gordon and Kral, 2019). Due to the high prevalence of developmental asymmetric hearing and the large portfolio of devices that can be used to alleviate hearing asymmetry [from hearing aids to cochlear implants (CIs)], asymmetric hearing during development has gained significant clinical attention (Gordon et al., 2015). To localize sound sources, subjects mainly rely on interaural time differences (ITDs) and interaural level differences (ILDs; Middlebrooks and Green, 1991;

Middlebrooks et al., 1994). Asymmetric hearing during development interferes with the ability to extract such cues. An aural preference syndrome following early-onset asymmetric hearing has been recently described (Gordon et al., 2015; Gordon and Kral, 2019), where single-sided hearing reorganized the developing auditory pathways toward the hearing ear, with weaker central representation of the deaf ear.

A mammalian model of congenital deafness is the congenitally deaf cat (CDC, Heid et al., 1998; Ryugo et al., 1998; Kral and Lomber, 2015). It provides the possibility of reversing deafness by chronic stimulation through a cochlear implantation (CI; Klinke et al., 1999; Ryugo et al., 2005). Rarely, congenital deafness in one ear and normal hearing in the other ear occur in this colony [unilaterally congenitally deaf cats (uCDCs), Kral et al., 2013b]. Using bilateral CI stimulation, this model allows for studying the developmental effects of congenital hearing loss in one or both ears (for review, see Kral et al., 2019). The standout advantage of the cat model is that it has excellent low-frequency hearing combined with a large head. This provides the animals with both ITD and ILD cues, making direct comparisons of the sensitivity to these cues possible.

In uCDCs, bilateral CI stimulation revealed a cortical aural preference reorganization toward the hearing ear, resulting in a "stronger" and a "weaker" ear (Kral et al., 2013a,b). Stronger representation of the hearing ear was observed in previous studies using neonatal unilateral cochlear ablation (Reale et al., 1987; Kitzes et al., 1995; McAlpine et al., 1997; Vale and Sanes, 2002; Vale et al., 2004). Cochlear ablation, however, precluded stimulation on the ablated ear. Using chronic CIs, an early critical period was documented for the aural preference change, i.e., it appeared only if hearing asymmetry set in before ∼4 months of age in cats (Kral et al., 2013a,b). The results correspond to those in sequentially implanted children, where a similar preference for the first implanted ear and a critical period has been documented (Gordon et al., 2013; Illg et al., 2013; Polonenko et al., 2017, 2018; Illg et al., 2019). When single-sided deaf children were implanted in the deaf ear, as expected, only interventions before 3 years of age provided sufficient benefit to the implanted ear (Sangen et al., 2019; Vanderauwera et al., 2020; Rauch et al., 2021). Deaf children with a delayed second cochlear implantation not only showed limited benefit of the second implant but also frequently became nonusers of the second implant (Myhrum et al., 2017) and showed a conflicting interference between the ears (Burdo et al., 2016).

Here, we asked how congenital binaural and single-sided deafness (SSD) affects ILD sensitivity in adult cats and how this ILD sensitivity compares to ITD sensitivity when using binaural cochlear implants. The results demonstrate the extensive effects of single-sided deafness on ILD sensitivity that is, in its impact on the representation of sound source location, different from the effect on ITD sensitivity. The reorganization of both binaural cues is consistent with the aural preference syndrome hypothesis. Additionally, in congenital single-sided deafness, we found an altered balance of excitation and inhibition of responses to the hearing and deaf ears in both hemispheres.

Materials and Methods

The present study was carried out on 22 adult cats. The experiments were approved by the local state authorities and were performed in compliance with the guidelines of the European Community for the care and use of laboratory animals (European Directive 2010/63/EU) and the German animal protection law.

Nine congenitally deaf cats (CDCs) were selected from a colony of deaf white cats using early hearing screening with auditory-evoked brainstem responses (ABR) and acoustic stimulation above 120 dB SPL (Heid et al., 1998). Using the same procedure, the animals' hearing status was additionally confirmed at the beginning of the acute experiments. Nine other animals had normal hearing (lowest hearing threshold, <40 dB SPL, detected using ABRs, Tillein et al., 2016). Four unilaterally congenitally deaf cats (uCDCs) used here were identified in the colony of deaf white cats during the hearing screening procedure. In these cases of a large binaural asymmetry of hearing thresholds, to prevent responses conveyed by bone conduction to the other side, the better-hearing ear was masked by an ongoing noise, and the absence of brainstem responses to the other ear demonstrated deafness of that ear (Tillein et al., 2016). This conclusion in uCDCs was finally confirmed in the acute experiments after deafening the hearing ear. The hearing condition thus corresponds to congenital single-sided deafness (SSD).

In part, the experimental methods are provided in detail elsewhere (Tillein et al., 2016) and will be only briefly recapitulated here.

Terminology. In what follows, the nine hearing-experienced animals with hair cells destroyed at the beginning of the acute experiment are referred to as hearing cats (HCs). The adjective "hearing" does not refer to the functional state of the cochlea during the experiment but to the developmental and functional state of the central auditory system.

Given the complex anatomical arrangements in uCDCs, we will use the following terminology as previously described (Kral et al., 2013a; Tillein et al., 2016):

1. The terms contralateral/ipsilateral always refer to the hearing ear in uCDCs. This means that the contralateral cortex is in the opposite hemisphere of the brain relative to the hearing ear. The hemisphere contralateral to the hearing ear is thus always denoted as $uCDC_c$, and the hemisphere ipsilateral to the hearing ear is always denoted as $uCDC_i$.
2. The terms crossed/uncrossed always refer to the cortical region recorded. The crossed ear is the ear on the head side opposite to the one that was recorded.

In consequence, if the left ear is hearing, the contralateral hemisphere is the right hemisphere. If the recording is on the ipsilateral (left) hemisphere in this animal, the crossed ear is then the right (deaf) ear.

Experimental procedures. All animals were initially anesthetized with intramuscular application of ketamine hydrochloride (24.5 mg/kg Ketavet, Parker Davis) and propionyl promazine phosphate (2.1 mg/kg Combelen, Bayer). After Combelen had been taken off the market, it was replaced by xylazine (1 mg/kg; WDT). All animals intraperitoneally received 0.25 mg atropine to reduce bronchial secretion. The animals were then tracheotomized and artificially ventilated with 50% O_2 and 50% N_2O, with the addition of a 0.2–2.0% concentration of isoflurane (Lilly) adjusted to maintain a controlled depth of anesthesia (Kral et al., 1999). End-tidal CO_2 was monitored and maintained below 5%, and the core temperature was kept above 37.5°C using a homeothermic blanket. The animal's status was further monitored by blood gas concentration measurements, pH, bicarbonate concentration and base excess, glycemia, and oxygen saturation determined from capillary blood. A modified Ringer's solution containing bicarbonate and plasma expander was infused (50 ml/kg/day, i.v.) with 5 µl atropine and additional bicarbonate, depending on the acid–base status. Monitoring and correction of the acid–base balance were performed every 12 h.

The animal's head was fixed in a stereotactic holder (Horsley–Clarke). Both bullae and ear canals were exposed. To record evoked auditory brainstem responses, we drilled a small trephination at the vertex and epidurally attached a silver ball electrode (diameter, 1 mm).

Hearing status was verified using ABRs in response to condensation clicks (50 µs) applied through a modified DT 48 speaker (Beyerdynamic). The speaker membrane was positioned ∼1 cm from the tympanic membrane within a custom-made, acoustically calibrated sound delivery device (closed system) inserted into the remaining part of the external auditory meatus after the pinna was removed. ABRs were recorded using an epidural vertex electrode compared with a

reference at the midline of the neck, were preamplified (60 dB, Otoconsult V2 low-impedance amplifier), amplified (40 dB, Otoconsult Amplifier-Filter F1; filters, 0.010–10 kHz), and recorded using National Instruments MIO cards. The signals were averaged (200 sweeps; repetition rate, 33 Hz; Audiology Lab, Otoconsult). The absence of acoustically evoked brainstem responses (including Wave I, generated within the auditory nerve) to clicks above 120 dB SPL verified complete deafness. In cases of large binaural asymmetry of hearing thresholds, the better-hearing ear was masked using an ongoing noise, and the absence of brainstem responses to the other ear demonstrated deafness in that ear. This result was confirmed after deafening the hearing ear (Hartmann et al., 1984). All hearing ears were deafened by slow instillation of 300 µl of neomycin sulfate into the scala tympani (within 5 min). The neomycin was left in place for a further 5 min and subsequently washed out by slow instillation of the Ringer's solution. The total absence of brainstem-evoked responses verified that the deafening procedure was successful.

For electrical stimulation, the animals were bilaterally implanted with a custom-designed feline cochlear implant (CI) electrode array in each cochlea inserted via the round window (cf. Tillein et al., 2016). To ensure insertion depth was comparable between the two ears relative to the stimulated neural elements, the electrode array was inserted until the most basal electrode of the implant entered the cochlea and a color mark on the implant was at the round window level (insertion depth, ~6 mm). The CI was secured with Histoacryl glue at the bulla wall, and the bulla opening was sealed with bone wax. Charge-balanced pulses (200 µs/phase; repetition rate, 2 Hz) were applied to the CI (wide bipolar stimulation; stimulation interelectrode distance, ~3 mm). Stimulation was performed with optically isolated current sources (CS1, Otoconsult).

Trephination was performed above the primary auditory cortex and the surrounding fields, and the dura was removed. The cortex was photographed to document the recording positions. Using an *x*–*y*–*z* micromotor (1 µm precision in all directions), a silver ball macroelectrode (diameter, 1 mm) was positioned at nine cortical positions on the primary auditory cortex (field A1) to determine the lowest cortical threshold to CI stimulation. The dorsal end of the posterior ectosylvian sulcus was used as a reference point. Signals [local field potentials (LFPs)] recorded in response to an electric biphasic pulse applied through a cochlear implant were preamplified (60 dB, Otoconsult V2 low-impedance amplifier), amplified at a second stage (20 dB, Otoconsult Amplifier-Filter F1; filters, 0.010–10 kHz), averaged (100 sweeps; repetition rate, 1.97 Hz), and recorded using National Instruments MIO cards. The signals were stored, and the threshold current levels were evaluated at all recording positions with a precision of ±1 dB.

To determine the extent of the activated cortical region and to define the cortical sites with the largest LFPs with CI stimulation, the surface of the auditory cortex was next mapped using microelectrodes with unilateral electrical stimulation on both the crossed and uncrossed ears at an intensity of 10 dB above the lowest cortical threshold determined with macroelectrodes (Kral et al., 2009). In all unilaterally deaf animals, recordings were performed on both hemispheres. After such functional activation maps in the cortex were determined, the cortical tissue was penetrated at the cortical spots with the largest LFPs ("hot spots") in field A1 (Kral et al., 2009) using a single-shank multielectrode array (NeuroNexus, single-shank, 16 contacts; spacing, 150 µm; contact area, 177 μm^2; electrode array length, 2.4 mm; impedance, ~1–2 MΩ) such that the last electrode was just at the level of the cortical surface. The movement of the cortex was stabilized using a modified Davies chamber filled with agar and sealed with melted bone wax.

The signals were amplified by a 64-channel Cheetah amplifier (NeuraLynx, amplified 5,000×; filters, 1 Hz–9 kHz), fed to the input of a National Instruments MIO card, digitized at a sampling rate of 25 kHz per channel, and stored on a computer using custom-made MATLAB routines. The signals were offline high-pass filtered (elliptic second-order IIR filter; edge frequency, 400 Hz), and stimulus artifacts were blanked. Zero-phase digital filtering was performed to avoid induced latency shifts. Multiunit activity was detected by an automatic thresholding procedure, and the thresholds were computed according to the formula:

$$\text{Threshold} = 3 \cdot \text{median}\left(\frac{|x|}{0.6745}\right), \quad (1)$$

where x is the high-pass filtered recorded signal and the constants were taken from a previous study on automated spike detection (Quiroga et al., 2004). At least three consecutive digital samples (duration, >80 µs) needed to be detected above the position threshold to be identified as a spike. The resulting spike trains were further analyzed.

Stimulation. Binaural stimulation was performed using cochlear implants in a wide bipolar configuration as described above. The responses to stimulation of each ear were first recorded separately with increasing intensity (1–2 dB current steps; interstimulus interval, 1,537 ms; biphasic charge-balanced pulses, 200 µs/phase). Subsequently, one ear was kept constant at 6 dB above the monaural threshold, whereas the other was increased from below the threshold up to 12 dB above the threshold, resulting in binaural stimulation that had varying average stimulation intensities. Since the average binaural intensity (ABI) here was variable, this paradigm will be called the ABI variable.

ILD stimulation under constant average binaural intensity (in what follows called "ABI constant") was performed using a train of three biphasic charge-balanced pulses (200 µs/phase) at a repetition rate of 500 pps, with reference to the individual EABR thresholds measured previously (Tillein et al., 2016). The current levels at both ears covaried from at least 1 dB below the threshold to at least 9 dB above the threshold. Increasing the current level at one ear was always compensated by decreasing the current level at the other ear so that the summed current level remained constant. Increases were made using 1 dB steps. Each stimulus condition was repeated 30 times so that robust averaged response properties could be determined. The total stimulation duration was <5 ms in all binaural conditions. To compensate for the possible differences, e.g., in the exact location of the cochlear implants within the scala tympani, we used the EABR threshold as a reference. Interaural time differences (ITDs) were pseudorandomly varied across the range from 0 to 600 µs (in 100 µs steps), with stimuli leading at either the ipsilateral or contralateral ear. ITD sensitivity was assessed at 5 ± 1 dB above the threshold levels. Each stimulus condition was repeated 30 times so that robust response properties could be measured. Interaural level differences (ILDs) were applied at a constant average binaural intensity corresponding to +6 dB relative to each EABR threshold.

Throughout the experiment, effective CI stimulation was verified by visual inspection of current monitor signals for both current sources (for both the contralateral and ipsilateral ears) using an oscilloscope. At the end of the experiment, current monitor signals were additionally recorded on the computer.

Data processing. Unit activity was analyzed in 0.5 ms windows, by which only one spike per window and durations of >70 µs were accepted. The firing rates per milliseconds were subsequently calculated using 1 ms bins. Poststimulus time histograms (PSTHs) were averaged from all animals and smoothed using a 3 ms sliding window. Since responses have a bimodal distribution in the PSTH often with complementary binaural responses (Tillein et al., 2010), we here confined the analysis to the first window (first 15 ms after the stimulus).

The units were considered to be responsive to the stimuli if the spike pattern in the analyzed poststimulus time windows could not be explained by a Poisson process (i.e., $p < 0.001$) using the spontaneous rate observed in the prestimulus time window (Chase and Young, 2007; Tillein et al., 2010). Probabilities were computed for all spikes in the time window analyzed. The unit was defined as responding to the stimulus if the probability that the spike train had been produced by a spontaneous Poisson process was <0.001. For binaural cues, responsiveness was accepted if three successive ITDs or ILDs were responded to significantly.

For the analysis of binaural interactions, first, the crossed ear was stimulated, and rate-intensity functions were measured. If not stated otherwise, the 6 ± 1 dB above threshold level was used, and the firing rates in the 15 ms after the stimulus were assessed and compared. Here, we represent the relation between the firing rate and varying interaural level as an ILD function, and correspondingly, the relation between the firing rate and varying interaural timing as an ITD function. In ILD functions, zero corresponds to equal levels above the thresholds on both ears, and positive ILDs correspond to higher levels at the crossed ear. In ITD functions, zero corresponds to a coincident stimulus, and positive ITDs correspond to crossed-ear earlier stimulation.

In the ABI variable condition, the crossed ear was constantly stimulated at 6 dB above the threshold, and the uncrossed ear with variable levels. For relative comparisons, the firing rates obtained at the given uncrossed stimulation level were normalized with reference to the firing rate with minimum variable stimulation level at the uncrossed ear (at 2 dB below threshold) and constant crossed-ear stimulation at 6 dB above the threshold (denoted as FR_{Mono}):

$$\text{Firing rate change} = \frac{\text{FR-FR}_{\text{Mono}}}{\text{FR}_{\text{Mono}}}, \quad (2)$$

where FR_{Mono} reflects the response to the crossed-ear stimulation to 6 dB above the threshold stimulation alone (effective monaural response, 6 dB) and FR reflects the response to the crossed-ear stimulation to 6 dB above the threshold combined with the given stimulation level at the uncrossed ear. The same calculation was performed under the conditions in which the stimulation at the crossed ear was variable and the one at the uncrossed was constant.

A Wilcoxon signed-rank test against zero was performed to establish whether a response corresponded to excitation from the variably stimulated ear to the constantly stimulated ear (if positive, i.e., FR increasing) or from inhibition (if negative, i.e., FR decreasing) (5% level, one-tailed). A nonsignificant difference to zero was considered as no interaction.

Statistics. All statistics were computed in MATLAB (MathWorks). Comparisons were performed with the two-tailed Wilcoxon–Mann–Whitney test with Bonferroni's correction where required. When the same quantities assessed in all four groups of animals were compared, we used the nonparametric Kruskal–Wallis test. Where Kruskal–Wallis yielded significant main effects, post hoc testing was performed using the Tukey–Kramer test. Statistical comparisons were always performed at a 5% significance level. If not stated otherwise, the results in the text are given as medians ± the median absolute deviation.

Results

Unit recordings were collected evenly from all cortical layers in the most responsive positions (hot spot) as measured in surface mapping of the cortical activity (Kral et al., 2009). The present results are from 608 unit recordings in HCs, 464 unit recordings in CDCs, and 378 unit recordings in uCDCs. In the HCs and CDCs, the responses were recorded from one cortical hemisphere, and in the uCDCs, due to its asymmetric nature of deafness, the responses were collected from both hemispheres, ipsilateral and contralateral relative to the hearing ear ($uCDC_i$ and $uCDC_c$, respectively). Two of the uCDCs were deaf in the right ear and two in the left ear. To assign responses to individual groups, the groups were consistently color-coded throughout the paper (Fig. 1*A*). Throughout the text, the blue color is reserved for HCs and the hearing ear, red for CDCs and the deaf ear, cyan for the contralateral hemisphere in uCDCs, and orange for the ipsilateral hemisphere in uCDCs.

The general characteristics of the responses and the ITD sensitivity of units to cochlear implant stimulation in congenitally deaf cats and single-sided deaf cats have been reported previously (Tillein et al., 2010, 2016). Here, we focus on the analysis of interaural level differences and compare it to ITD sensitivity. We used two ILD paradigms: one in which both current levels were systematically modified with the average binaural intensity level in dB kept constant (ABI constant) and the other in which one ear was stimulated at the constant level of 6 dB above the response threshold and, in the other ear, the stimulation intensity was varied (ABI variable).

Unit responses to binaural stimulation often consisted of a sequence of two distinct responses with different tunings (Fig. 1*B*; for details with ITDs, see Tillein et al., 2010). To acquire consistent onset ITD and ILD responses, if not stated otherwise, we quantitatively analyzed here the response within the first 15 ms following stimulation onset (Fig. 1*B*).

Binaural stimulation under ABI constant condition: individual examples

We will first present individual examples of units of binaural stimulation and, subsequently, perform the statistical analysis of the data. To study the sensitivity to ITDs, the stimulation was at 6 dB above the threshold at each ear. In ILD, the initial stimulation was at 6 dB above the threshold at each ear, and this was subsequently modified keeping the binaural average intensity constant. In hearing controls, the majority of units showed a stronger response to the crossed-ear earlier and crossed-ear stronger condition when studied in the same units for ITD and ILD condition, respectively (Fig. 2). In binaurally deaf animals, the tuning remained unchanged (crossed-ear preference), although the modulation depth of both the ITD and ILD functions was reduced. The firing rate was smaller than that in the hearing controls (for ITD, cf. Tillein et al., 2010, 2016).

In animals with single-sided hearing, ITD functions were flat, i.e., showing only a small variation with changing ITD

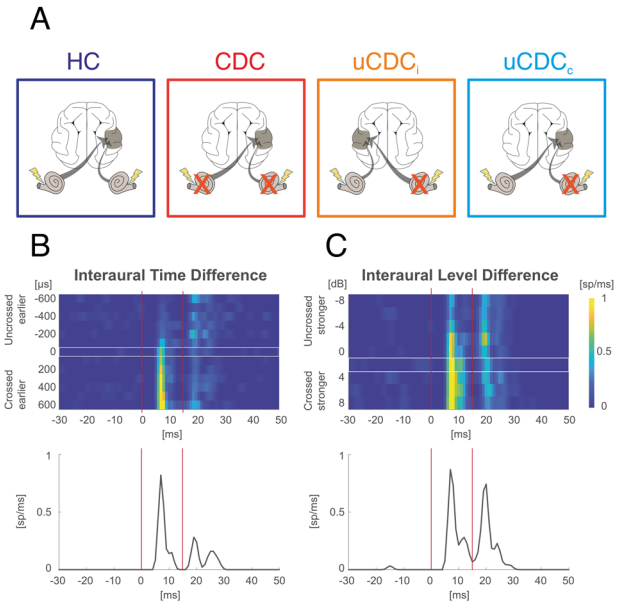

Figure 1. Group color coding and response analysis window. ***A***, Color coding of the investigated groups and hemispheres. Example unit response in an HC to stimuli with varying ITDs (***B***) and ILDs (***C***) and the underlying poststimulus time histograms (below) for ITD = 0 µs and ILD = 2 dB (white rectangle in color plots). The response is observed in two separate poststimulus periods, one within 0–15 ms, and the other, smaller in response magnitude, between 15 and 50 ms. Since they often have complementary tuning to binaural cues (Tillein et al., 2010), only the first response window (0–15 ms, marked by red vertical lines) was analyzed throughout the present study.

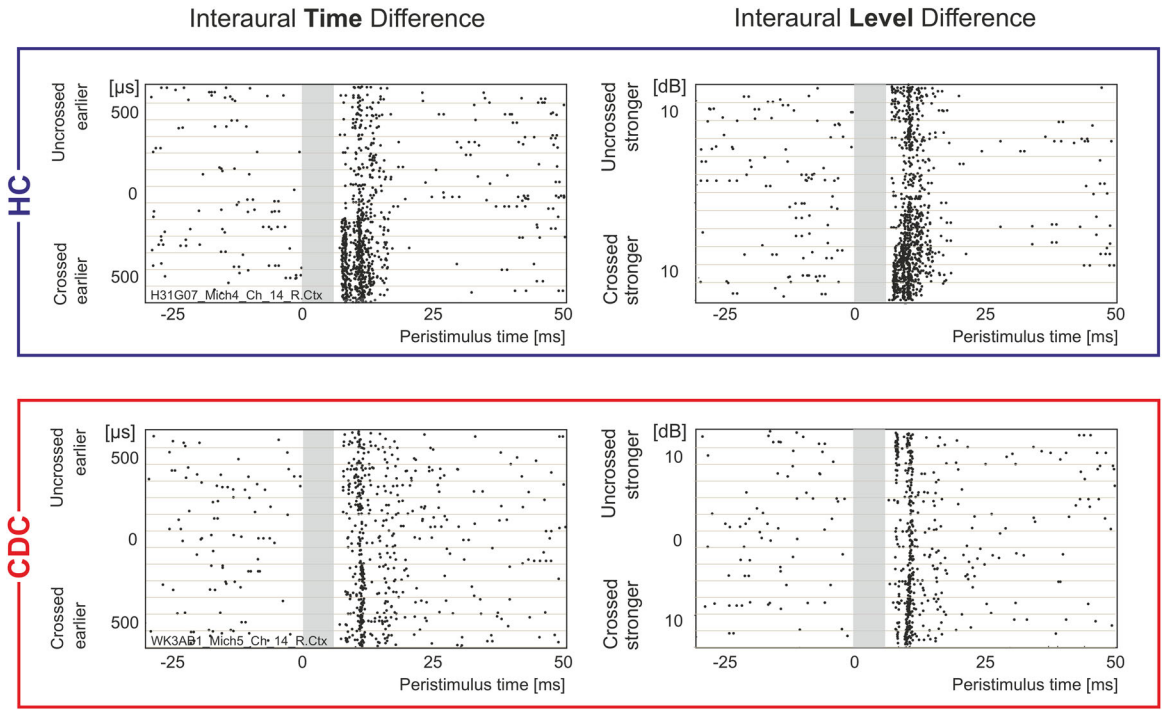

Figure 2. Example raster plots from representative units in one hearing control (top) and one congenitally (binaurally) deaf cat (bottom). Shown are the sensitivity to interaural time differences (left) and interaural level differences (right) of the same unit. In the hearing control, the unit responded preferentially to crossed-earlier and crossed stronger conditions. In the deaf cat, the responsiveness to both ITD and ILD was reduced and more similar for both crossed and uncrossed stimulation. The gray bar corresponds to the blanked region of the stimulus artifact. For a detailed analysis of the ITD responses in HCs and CDCs, see Tillein et al. (2010).

(Tillein et al., 2016). ILD responses in the same units, however, demonstrated a different behavior: response strength depended on the history of previous hearing experience, favoring the experienced (hearing) ear. To document this, Figure 3 shows the example units from two uCDCs where the hearing ear was on different sides. When hearing was present in the right ear (as observed in two uCDCs), the right-ear responses were strong and the left-ear responses were weak (Fig. 3*A*).

In the other two uCDCs with the other (left) ear hearing, there was a similar difference in the tuning to changing ITDs and ILDs (Fig. 3*B*): the ITD function was similarly flat, and ILD substantially modulated in favor of the hearing ear. In total, the response to the hearing ear was generally stronger than the response to the deaf ear at both hemispheres in uCDCs, which was different from the control groups where the response was stronger to the crossed ear (for statistics, see below). Furthermore, there was a dissociation of the ITD and ILD sensitivity in uCDCs.

Binaural stimulation under ABI constant condition: group analysis

Subsequently, to compare cortical representations of the binaural cues between the studied groups, we pooled all responses. We first computed the mean ITD and ILD sensitivity functions to obtain an overall measure of the sensitivity to these cues. In uCDCs, we pooled the units from both hemispheres (for hemispheric specificity, see below).

For ITDs, the previously described preference of the units for the crossed ear in HCs (Tillein et al., 2016), where crossed-ear earlier resulted in higher firing rates than uncrossed-ear earlier, was replicated in HCs (Fig. 4*A*). In CDCs (Fig. 4*B*), ITD functions showed a small but consistent increase in the mean response from uncrossed-ear earlier to crossed-ear earlier. This result also confirmed decreased modulation of ITD functions in CDCs (Tillein et al., 2010, 2016). In uCDCs, flat ITD functions were found (Fig. 4*C*). To statistically evaluate the ear preference within each group, we pooled ITDs within the range from −100 to 100 µs and compared these to more-negative and more-positive ITDs, resulting in three different configurations: uncrossed earlier, coincident, and crossed earlier. The results revealed significant differences only within the group of hearing cats (Fig. 4*A*), where the uncrossed-earlier condition revealed significantly lower firing rates compared with that in the coincident condition (Table 1, two-tailed Wilcoxon–Mann–Whitney test, $p = 5.7 \times 10^{-9}$) and the firing rate was also smaller than in crossed-earlier condition (Table 1, two-tailed Wilcoxon–Mann–Whitney test, $p = 3.6 \times 10^{-10}$).

The pooled ILD sensitivity functions (Fig. 4*D*) revealed a systematic increase in firing rate from uncrossed stronger, through balanced, to the crossed stronger conditions in HCs (Table 1 and Fig. 4*D*; significant differences, two-tailed Wilcoxon–Mann–Whitney test, $p < 0.05$). In CDCs, this trend was partially present (Fig. 4*E*), with the uncrossed stronger condition leading to lower firing rates compared with balanced (two-tailed Wilcoxon–Mann–Whitney test, $p = 0.001$) and crossed stronger conditions (two-tailed Wilcoxon–Mann–Whitney test, $p = 4.5 \times 10^{-4}$). In uCDCs, this effect could not be found (Fig. 4*F*; Table 1). For within-group statistical analysis, we pooled ILDs within ±2 dB around the balanced condition and compared this to the firing rates at more-positive and more-negative ILDs in all three groups of animals (lower panels). While significant differences showed up in both control groups, they were not observed in uCDCs.

In CDCs, ITD functions with no difference between coincident, uncrossed-earlier, and crossed-earlier conditions

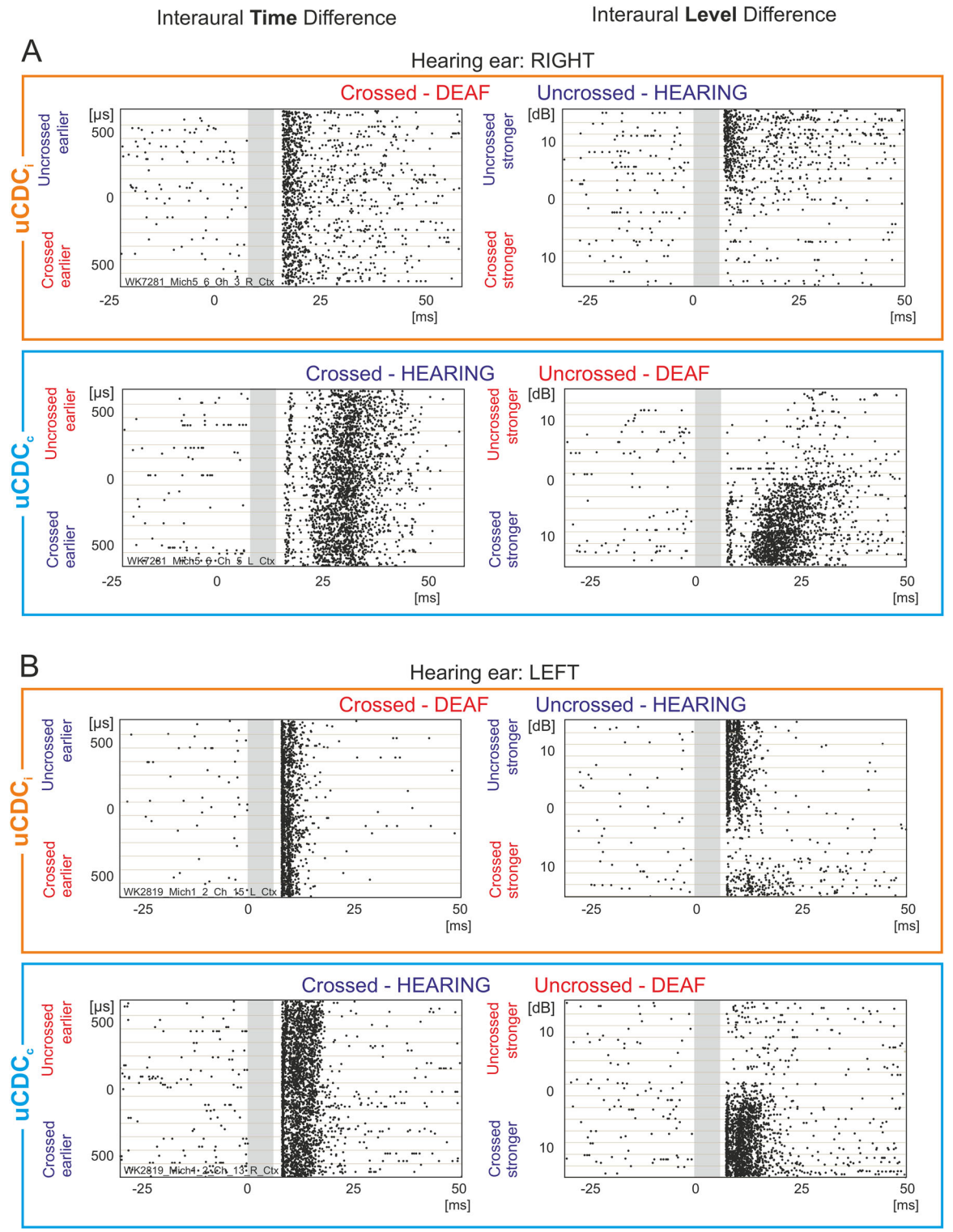

Figure 3. Representative unit responses in two uCDCs (one with the right, the other with the left hearing ear) showing flat ITD function and ILD tuning favoring the hearing ear irrespective of recording hemisphere. ***A***, Responses to binaural cues for the hearing ear on the right side, recorded either from the ipsilateral ($uCDC_i$, top) and contralateral ($uCDC_c$, bottom) cortices. The ITD (left) and ILD (right) results were both from the same unit. While ITDs in both hemispheres showed a flat ITD sensitivity response, the ILDs resulted in a strongly preferred ear—the hearing ear (blue legend). The response to the deaf ear (red legend) was weak. Note that the comparison within the same hemisphere is for the same unit. ***B***, Representative unit responses in an uCDC with left-ear hearing, recorded at the ipsilateral (top) and contralateral (bottom) cortices, respectively, in response to its hearing (blue) and deaf (red) ear earlier or stronger.

(Fig. 4*B*) thus confirmed a reduced modulation depth (less dependence of the evoked firing rate on the crossed/uncrossed condition) compared with the HCs that showed significant differences in same comparisons (Fig. 4*A*). In uCDCs, ITDs and ILDs were not sensitive to changes in the crossed/uncrossed condition (Fig. 4*C*). However, a notable finding was a higher mean firing rate in the binaural condition in uCDCs.

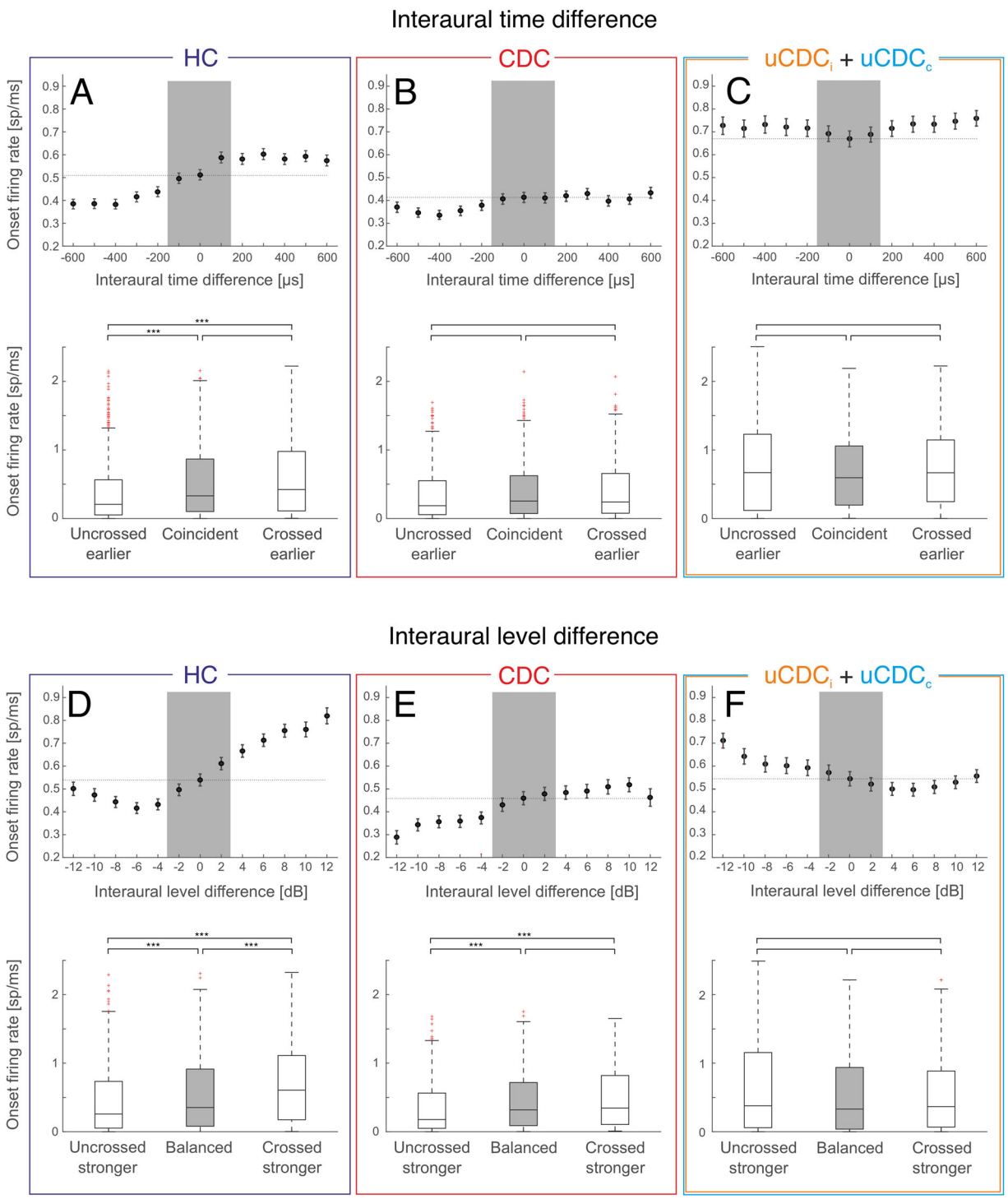

Figure 4. Grand mean ITD and ILD functions of all responsive units recorded in the study. ***A–C***, Grand mean ITD function (mean ± standard errors; top panels) and pooled ITD data for uncrossed-earlier (less than −100 μs), balanced (−100 to +100 μs), and crossed-earlier (greater than −100 μs) condition (bottom panels). In hearing controls (***A***, blue frame), the firing rate significantly increased from uncrossed-ear earlier to crossed-ear leading stimulation. In congenitally deaf cats (***B***, red frame), the functions showed a small constant increase from uncrossed to crossed condition; however, it did not reach statistical significance. In uCDCs (***C***, pale blue/yellow frame), ITD functions were flat, however, at a higher overall firing rate than in CDCs. The dashed line depicts the overall mean firing rate in top panels, and the gray rectangles encompass the ILDs defined as "balanced" conditions. Two-tailed Wilcoxon–Mann–Whitney test with multiple comparisons corrected using Bonferroni's procedure in bottom panels, ***$\sim p < 0.001$. ***D–F***, Grand mean ILD functions (mean ± standard errors; top panels) and pooled ILD data for uncrossed stronger (less than −2 dB), balanced (−2 to +2 dB), and crossed stronger (greater than −2 dB) condition (bottom panels). In hearing controls (***D***, blue frame), the firing rate increased with crossed-ear stronger stimulation (positive ILDs) and decreased with uncrossed-ear stronger stimulation. Pooling all data from balanced ILD conditions and comparing them with more-negative ILDs (uncrossed stronger) resulted in a significant difference, and the comparison to the more-positive ILDs (crossed stronger) was also statistically significant. In congenitally deaf cats (***E***, red frame), a significance was observed in the comparison between balanced and uncrossed stronger, as well as the uncrossed stronger to crossed stronger condition. In uCDCs (***F***, pale blue/yellow), the mean ILD function was flat. Correspondingly, no effect was observed in the statistical analysis. Two-tailed Wilcoxon–Mann–Whitney test with multiple comparisons corrected using Bonferroni's procedure, ***$\sim p < 0.001$.

Table 1. Means ± standard deviations of the peak firing rates (spikes/ms) corresponding to Figures 4 and 5

ITD	Uncrossed earlier	Centered	Crossed earlier
Hearing controls	0.40 ± 0.02	0.52 ± 0.02	0.58 ± 0.02
Congenitally deaf	0.36 ± 0.02	0.41 ± 0.02	0.42 ± 0.02
Single-sided deaf	0.71 ± 0.04	0.69 ± 0.03	0.74 ± 0.03
ILD	**Uncrossed stronger**	**Balanced**	**Crossed stronger**
Hearing controls	0.45 ± 0.02	0.54 ± 0.03	0.69 ± 0.03
Congenitally deaf	0.35 ± 0.03	0.46 ± 0.03	0.50 ± 0.03
Single-sided deaf	0.63 ± 0.03	0.55 ± 0.03	0.52 ± 0.03
ITD	**Deaf earlier**	**Centered**	**Hearing earlier**
SSD by ear	0.72 ± 0.04	0.69 ± 0.03	0.73 ± 0.03
ILD	**Deaf stronger**	**Balanced**	**Hearing stronger**
SSD by ear	0.46 ± 0.03	0.55 ± 0.03	0.68 ± 0.03

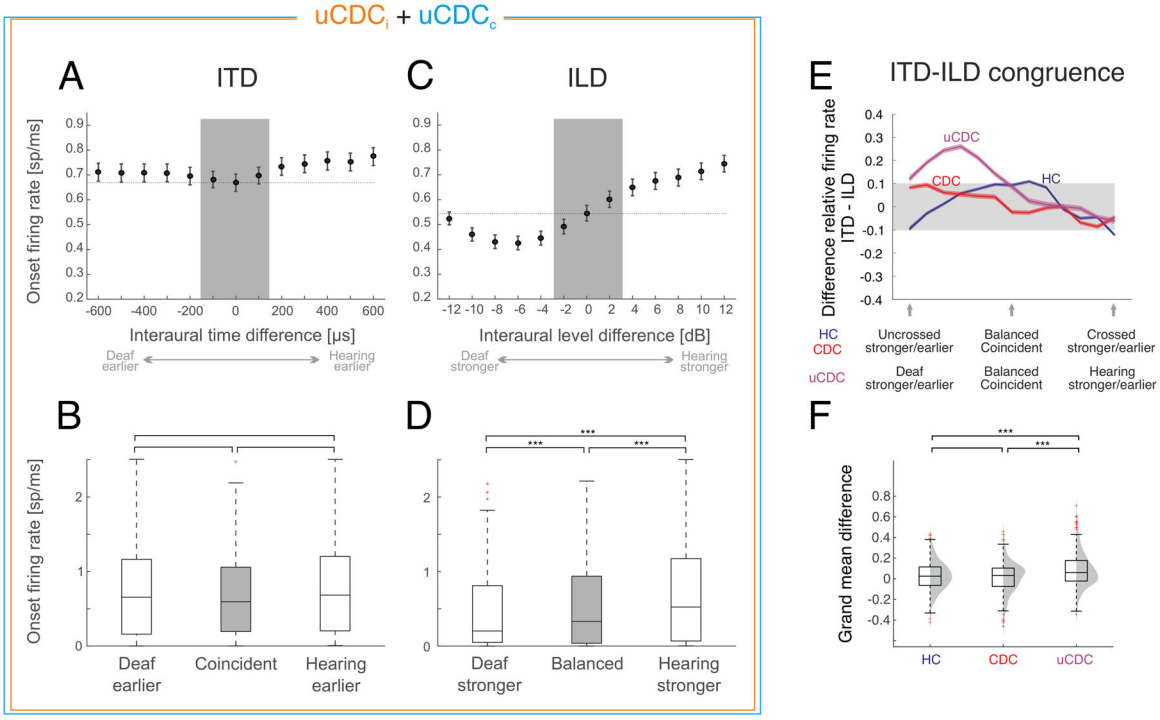

Figure 5. Representations of binaural cues in uCDCs resorted relative to the deaf and the hearing ear. Grand mean ITD and ILD functions shown as mean ± standard error. ***A***, ***B***, Pooling the results relative to the hearing and deaf ears did not reveal any significance in ITD sensitivity, similar to the crossed/uncrossed alignment. Sorting the ILD sensitivity relative to the hearing and deaf ears (***C***, ***D***), however, changed the mean ILD function substantially. Here, the deaf ear stronger condition resulted in a weaker response, whereas the hearing ear stronger condition resulted in a stronger response, generating an ILD tuning preferring the previously hearing ear. Correspondingly, all differences in statistical comparisons were significant in such resorted ILD functions (***D***). ***E***, Pairwise differences in the subset of units (see text) that showed sensitivity to both ITD and ILD. The firing rates were normalized to the maximum of each function. Shown are the grand mean ITD–ILD differences ± standard errors of the mean. Only the uCDC data show several successive data points in the grand mean well beyond 0.1 relative difference (pale gray horizontal stripe). ***F***, Statistical comparison between the mean difference values, demonstrating a systematic difference between ITD and ILD tuning only in uCDCs. Two-tailed Wilcoxon–Mann–Whitney test, multiple comparisons corrected by Bonferroni's procedure, ***$\sim p < 0.001$.

ILD representations in uCDCs are dominated by the hearing ear

We subsequently sorted all ILD and ITD data based on the condition of the ear (deaf-earlier/hearing-earlier and deaf-stronger/hearing-stronger conditions) in uCDCs. In the resorted grand mean, the ITD functions were similarly flat (Fig. 5*A*), with no significant differences between crossed-earlier, balanced, and uncrossed-earlier conditions (Fig. 5*B*). However, sorting the ear depending on the hearing status resulted in a significant ILD effect: increasing the current level at the deaf ear (while reducing it at the hearing ear) reduced the firing rate, and increasing the current level at the hearing ear (while reducing it at the deaf ear) increased it (Fig. 5*C*). The effect was significant both with respect to the balanced condition, as well as with respect to the hearing ear stronger condition (Fig. 5*D*, Table 1).

The pooled ILD and ITD functions allowed us to perform statistical testing, but pairwise comparisons were precluded due to the criteria of binaural responsiveness (since one of the ITD and ILD functions in some cases did not meet the criteria of a systematic response; see above, Materials and Methods). To examine the relation between ITD and ILD sensitivity, we also performed pairwise comparisons in a subgroup of units that were responsive both to

ILD and ITD (responsiveness was given if at least three neighboring ITD and ILD values were significantly responded to) and thus could be directly pairwise-related (HCs, 369 units; CDCs, 220 units; and uCDCs, 241 units). We first normalized each function so that the maximum firing rate was 1 and then subtracted the normalized ILD sensitivity function from the normalized ITD sensitivity function (to match the range of physiological ILDs and ITDs with electric stimulation of ~8 dB and 400 µs, corresponding to 1 dB step of ~50 µs delay). In the grand mean, uCDCs showed the largest peak in the difference function (Fig. 5*E*, top panel). Subsequently, the grand means of all these data were then pooled in each animal group and compared (Fig. 5*F*). The uCDCs showed significant differences to both HCs and CDCs, while the latter groups were not different (Wilcoxon–Mann–Whitney test, $p < 0.05$). This further supports more consistent ITD–ILD tuning in both controls compared with uCDCs.

It is likely that the responses in both hemispheres were mainly determined by the previously hearing ear in uCDCs, explaining the dissociation between the effect of SSD on ITDs and ILDs. The ILD findings in uCDCs with a reduced firing in the deaf-stronger condition might suggest a suppressive effect on the deaf ear. However, with constant average binaural intensity, the result can also be due to a reduced stimulation level of the previously hearing ear. Therefore, to clarify the quality of binaural interactions, in a second paradigm, we further abandoned the constant average binaural intensity and focused on binaural facilitation and suppression.

Binaural stimulation under ABI variable condition: effect of the recorded hemisphere

After having determined the responses to the monaural crossed ear (Fig. 6*A*), we kept the crossed ear at the level 6 dB above the threshold and added the stimulation at the uncrossed ear with increasing current level (Fig. 6*B*). Increasing the stimulation level at the uncrossed ear allowed us to directly observe its effect on the response to the crossed ear and, by that, to differentiate excitatory and inhibitory interactions in binaural stimulation.

As expected, adding the uncrossed ear in HCs increased the firing rate in some units, in others, it decreased it or had no effect. We normalized the response relative to the −2 dB condition (Fig. 6*C*, −2 dB condition: 6 dB above the threshold at the crossed ear and 2 dB below the threshold at the uncrossed ear, in what follows called effective monaural crossed stimulation). By comparing the pooled firing rates (for all current levels) to zero, we could then statistically test whether the response of the individual unit significantly decreased (<0) or increased (>0) with increasing uncrossed current level (Fig. 6*C*). We could then identify the proportion and strength of significant excitatory and significant inhibitory interactions in all three groups of animals.

To quantify the number of excitatory and inhibitory interactions, we used the statistical comparison of the modulatory effect as shown in Figure 6, *B* and *C*, and examined whether the mean firing rate change for each unit over all uncrossed

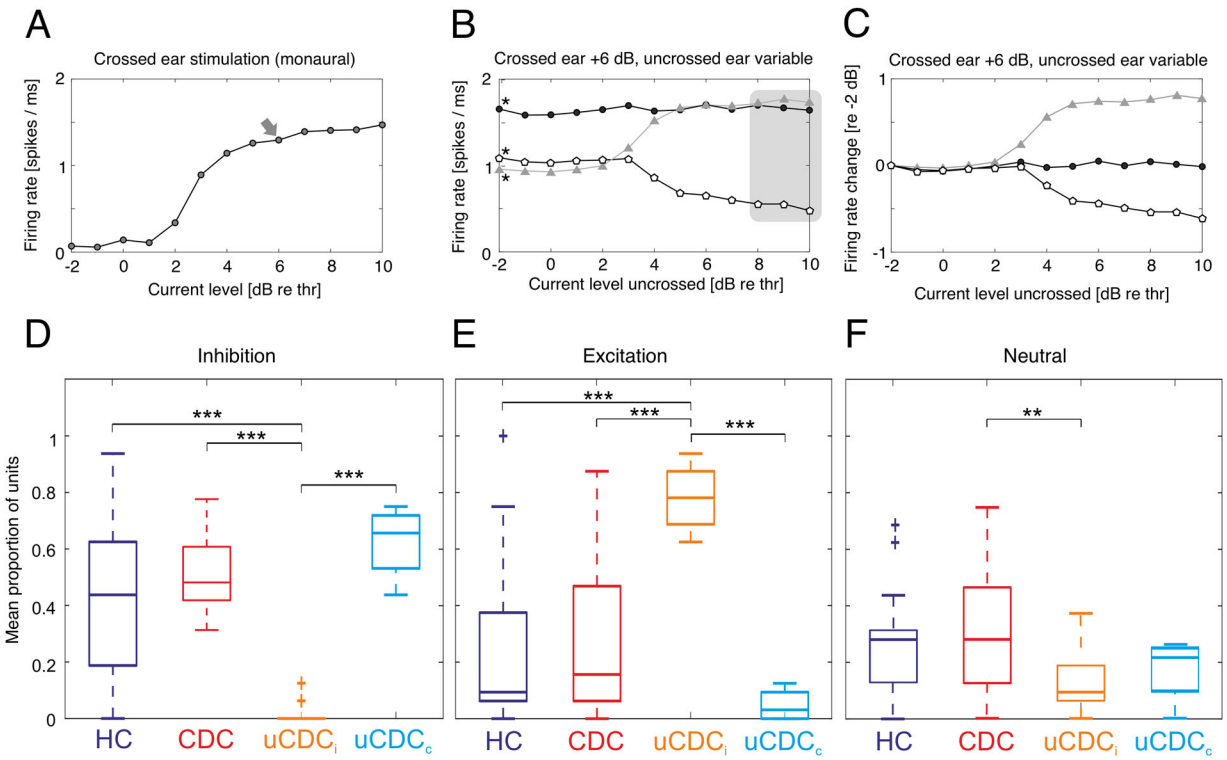

Figure 6. Variable ABI paradigm focused on the analysis of excitation–inhibition balance. ***A***, An individual unit example from an HC shows a monotonically increasing firing rate with an increasing current level. The arrow shows the +6 dB condition. ***B***, Adding the uncrossed ear to the crossed-ear stimulation at 6 dB resulted either in an unchanged firing rate (black bullets, neutral interaction), an increasing firing rate (gray triangles, excitatory interaction), or a reduced firing rate (white pentagons, inhibition). The −2 dB stimulation at the uncrossed ear and +6 dB at the crossed ear (denoted by the asterisks) defines the "−2 dB condition" and corresponds to a response to an effective crossed stimulation with 6 dB. The mean of +8, 9, and 10 dB above the threshold at the uncrossed and +6 dB at the crossed ear (gray rectangles) will be termed as "binaural maximum" in subsequent text. ***C***, Relating the firing rate to the −2 dB condition clearly sorts the neutral, excitatory, and inhibitory interactions. Statistical comparison (Wilcoxon–Mann–Whitney test, $\alpha = 5\%$) of all pooled values relative to zero for each unit response allows us to define excitation, inhibition, and neutral interactions. ***D***, Statistical comparison of the proportion of the recording sites (units) expressing excitation and inhibition. Binaural inhibition was typically observed by ~40% of the units in HCs. In uCDC$_i$, there were essentially no inhibitory interactions, whereas in uCDC$_c$, these were not different from HCs. ***E***, The results for excitation were reciprocal to those of inhibition in uCDCs. ***F***, Neutral interactions showed only a significant difference between CDCs and uCDC$_i$. Kruskal–Wallis test with Tukey–Kramer post hoc significance difference criterion. *~$p < 0.05$; **~$p < 0.01$; ***~$p < 0.001$.

levels was significantly smaller (pentagons) or larger (triangles) than zero. The interaction was classified as excitatory or inhibitory only if the significance level was reached. Subsequently, the proportion of units with significant excitatory and inhibitory interactions per penetration was compared (Fig. 6*D*,*E*). Such a view ignores the strength of these effects (analyzed below) but instead considers the type (quality) of interaction. Inhibitory interaction showed a significant main effect on the groups (Kruskal–Wallis test, $p < 0.001$). HCs and CDCs did not differ in the relative number of inhibitory interactions (HCs, 0.44 ± 0.24; CDCs, 0.25 ± 0.17; post hoc Tuckey–Kramer test, $p = 0.4123$). However, $uCDC_i$ showed a complete loss of inhibitory interactions, whereas $uCDC_c$ showed a normal level of inhibitory interactions ($uCDC_i$, 0.0 ± 0.03; $uCDC_c$, 0.66 ± 0.09; Kruskal–Wallis test with post hoc Tuckey–Kramer test, $p = 0.0002$). The corresponding results were obtained from excitation (Fig. 6*E*, Kruskal–Wallis test, $p < 0.001$). Excitation was overrepresented in $uCDC_i$ while only a small proportion of excitatory interactions was observed in $uCDC_c$. While there were significant differences between the proportion of neutral interactions (Kruskal–Wallis test, $p = 0.009$), the post hoc testing revealed only a significant difference between CDCs and $uCDC_i$ ($p = 0.006$). No interactions were observed in all groups in ~10% of units, and no significant differences were also observed between the groups (Kruskal–Wallis test, $p = 0.76$).

Consequently, nearly all units receiving a crossed projection from a deaf ear could be excited ($uCDC_i$) by an uncrossed projection from a hearing ear, whereas a majority of the units (~60%) receiving a crossed projection from a hearing ear could be inhibited by an uncrossed projection from a deaf ear ($uCDC_c$).

Further, the strength of excitation and inhibition was evaluated (Fig. 7). In Figure 7*A*, the grand mean PSTH responses are presented. As expected, the grand mean average PSTHs at −2 dB below the threshold (effective monaural crossed stimulation) showed the strongest response in HCs and at the contralateral cortex in uCDCs ($uCDC_c$, Fig. 7*A*). Adding the uncrossed ear to the stimulation tended to decrease the mean response in HCs and CDCs (Fig. 7*B*). Adding the uncrossed ear at the cortex ipsilateral to the hearing ear in uCDCs ($uCDC_i$) increased the peak firing rate in $uCDC_i$ only but decreased it at the cortex contralateral to the hearing ear ($uCDC_c$). This means that in uCDCs increasing the current level at the hearing ear increased the firing rate, yet increasing the current level at the deaf ear decreased it.

We calculated the difference between the mean of the three largest current levels in binaural stimulation and the −2 dB condition (Fig. 7*C*). In both HCs and CDCs, there was an initial

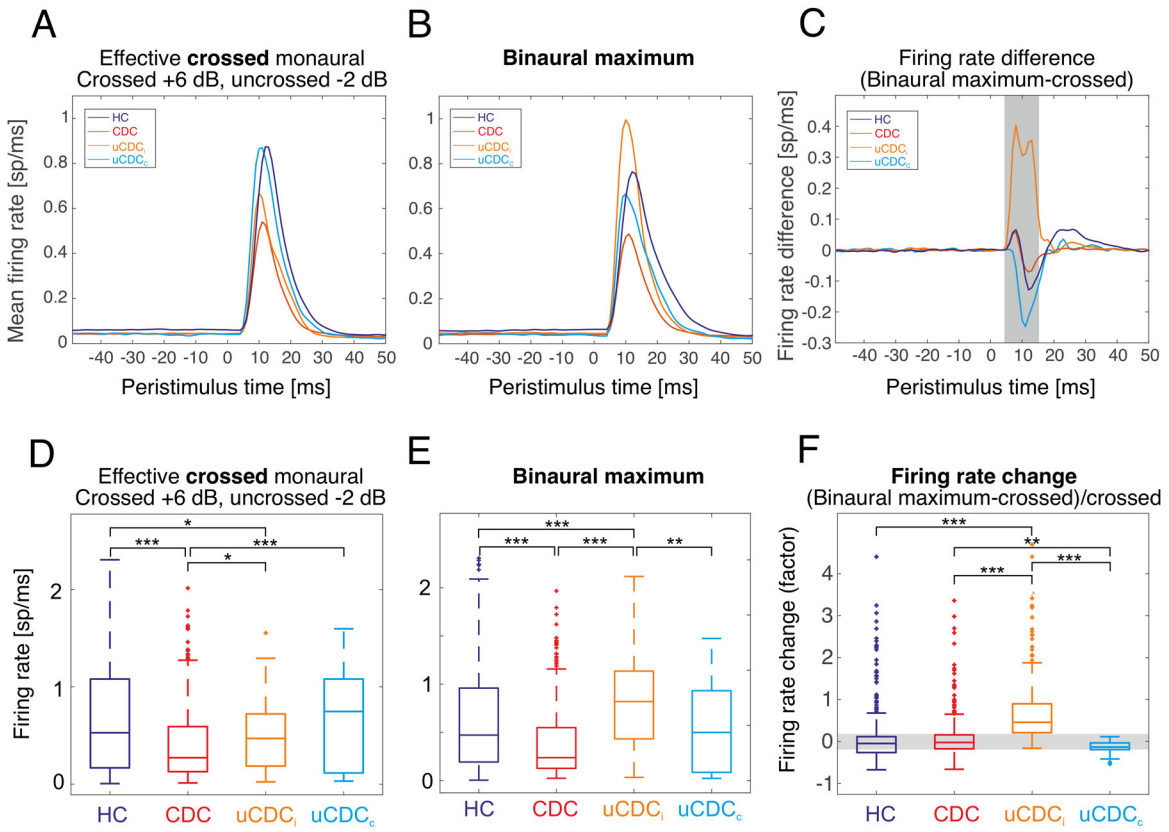

Figure 7. ABI variable paradigm results. ***A***, The mean response from all units at 6 dB (above the threshold) at the crossed ear and −2 dB (below the threshold) at the uncrossed ear. HCs and $uCDC_c$ demonstrated strong responses, while CDCs and uCDCi showed the weakest. ***B***, Increasing the uncrossed level to the maximum current substantially increased the uCDCi response, whereas the HCs and $uCDC_c$ responses tended to be suppressed. ***C***, The firing rate change (difference between the mean firing rate of the three largest current levels and the firing rate at −2 dB level) illustrates that in both HCs and CDCs, there was a mixed excitation–inhibition effect, whereas the $uCDC_i$ showed a mean excitation and $uCDC_c$ showed a mean inhibition. The gray rectangle shows the 15 ms that were evaluated for firing rate analysis. ***D***, Firing rate at 6 dB above the threshold at the crossed ear and −2 dB at the uncrossed ear. The highest firing rates were confirmed for HCs and $uCDC_c$. ***E***, Same data for the maximum current level at the uncrossed ear and 6 dB at the crossed ear. ***F***, Analysis of the change in firing rate. The gray rectangle shows the ±0.2, the margin around zero that is considered the "occlusion" or "neutral" interaction (Tillein et al., 2016). It shows that in three-quarters of the units in $uCDC_i$, the excitation was beyond that margin and thus represents a genuine excitatory effect. In $uCDC_c$ (as in HCs), the suppression was in approximately half of the units within the "occlusive" margin and only ~25% in the suppression range, suggesting that the strength of inhibition is moderate. Kruskal–Wallis test with Tukey–Kramer post hoc significance difference criterion, *~$p < 0.05$; **~$p < 0.01$ and ***~$p < 0.001$.

increase in response followed by a decrease; however, in uCDCs, there was a hemispheric-specific effect. At the hemisphere contralateral to the hearing ear, a response decrease in the binaural condition was observed, and at the ipsilateral hemisphere, there was a strong increase in response.

Further, we have statistically compared effective monaural responses (Fig. 7*D*; HCs, 0.53 ± 0.45 spikes/ms; CDCs, 0.27 ± 0.30 spikes/ms; $uCDC_i$, 0.47 ± 0.30 spikes/ms; $uCDC_c$, 0.75 ± 0.44 spikes/ms; Kruskal–Wallis test, $p < 0.001$). Post hoc Tukey–Kramer test revealed that all groups differed significantly, except for HCs versus $uCDC_c$ ($p = 0.68$). The uCDCs thus had a higher firing rate compared with the CDCs of both hemispheres, and at the hemisphere contralateral to the hearing ear, they were even comparable to the hearing controls.

The firing rates in the binaural condition—at maximum current levels with uncrossed ear and +6 dB with the crossed ear—also confirmed significant differences (Fig. 7*E*; HCs, 0.47 ± 0.41 spikes/ms; CDCs, 0.24 ± 0.29 spikes/ms; $uCDC_i$, 0.82 ± 0.39 spikes/ms; $uCDC_c$, 0.50 ± 0.39 spikes/ms; Kruskal–Wallis test, $p < 0.001$). In this case, the post hoc Tukey–Kramer test revealed that all differences were significant, except HCs versus $uCDC_c$ ($p = 0.7802$) and CDCs versus $uCDC_c$ ($p = 0.068$).

Since both these measures (effective monaural and maximum binaural) revealed differences between groups, we additionally computed a ratio of the two. Since the firing rate at the −2 dB condition (driven by +6 dB from the crossed ear) was the denominator, a value of −0.5 corresponded to a 50% reduction of the firing rate of the crossed response by the uncrossed ear. In HCs and CDCs, both excitatory and inhibitory responses were observed, with medians in the negative range (Fig. 7*F*; HCs, −0.05 ± 0.34; CDCs, −0.02 ± 0.29, not significantly different, Kruskal–Wallis test with Tukey–Kramer post hoc significance difference criterion, $p = 0.2798$). The shaded region between −0.2 and 0.2 (Fig. 7*F*) is considered occlusion or neutral interaction (Smith and Delgutte, 2007; Tillein et al., 2016) and does not provide clear evidence of excitation or inhibition. While the range of observed firing rates was larger in HCs than that in CDCs, the mean difference was not significant, indicating a balanced excitation and inhibition in the overall population of units in both HCs and CDCs. The two hemispheres in uCDCs differed from each other in the firing rate change (Kruskal–Wallis test with Tukey–Kramer post hoc significance difference criterion, $p < 0.001$): the hemisphere contralateral to the hearing ear exhibited preferential reduction of firing rate relative to the −2 dB condition (median, −0.13 ± 0.10), with >25% of the neurons in the true suppressive region of less than −0.2 and ∼50% of the neurons in the region of occlusion. In contrast to the other hemisphere, no units showed excitation (>0.2). On the other hand, at the hemisphere ipsilateral to the hearing ear, the interactions were mainly excitatory (median, 0.46 ± 0.55) and no units were in the inhibitory region (less than −0.2). Subsequently, the units showing inhibition were compared between groups to assess the inhibition strength: the groups differed significantly ($p = 2.21 \times 10^{-6}$). Post hoc tests showed that the inhibition (quantified by the maximum reduction of the firing rate due to stimulation at the uncrossed ear) observed at the contralateral cortex ($uCDC_c$) was weaker than that in HCs (HCs, −0.24 ± 0.17; $uCDC_c$, −0.17 ± 0.13, $p = 0.035$) and not different from CDCs (CDCs, −0.19 ± 0.14, $p = 0.857$).

In total, Figures 6 and 7 reveal the hemispheric difference: we observed mostly excitatory effects of the hearing ear whereas mostly suppressive effects of the deaf ear at the contralateral hemisphere in $uCDC_c$. The excitation was significantly stronger than in the HCs and CDCs, whereas the inhibition was in the range of HCs and CDCs.

Binaural stimulation under ABI variable condition: effect of the stimulated ear

In the previous section, when analyzing the contralateral cortex, the uncrossed ear was always the deaf ear in uCDCs. When analyzing the ipsilateral cortex, the uncrossed ear was always the hearing ear. Was the observed difference in the interactions due to the recorded hemisphere or due to the effect of the hearing and deaf ear?

To answer this question, we have considered the responses from both cortical hemispheres in uCDCs with both the hearing or the deaf ear variable (and the other ear constant at 6 dB) in a subset of 288 units (Fig. 8*A*,*B*). Such ILD functions were subsequently grouped into those showing an increase and decrease in firing rate, which enabled us to analyze the excitatory and inhibitory effects of the hearing and deaf ears, respectively. Statistical comparison revealed an excessive excitatory effect of the hearing ear (proportion of the cortical positions for the hearing ear effect: excitation, 86.2 ± 13.8%; inhibition, 13.8 ± 2.4%; deaf ear effect: excitation, 21.9 ± 8.3; inhibition, 78.1 ± 8.3%; Wilcoxon–Mann–Whitney test, $p < 0.001$; for distribution within the two hemispheres, see pie charts in Fig. 8*A*,*B*) as well as in the strength of the excitation (hearing ear effect: excitation, 0.434 ± 0.033; inhibition, 0.079 ± 0.016; deaf ear effect: excitation, 0.106 ± 0.025; inhibition, 0.126 ± 0.015; Kruskal–Wallis test, $p < 0.001$). The deaf ear thus expressed a weak excitatory effect in proportion and strength when compared with the hearing ear (Fig. 8*C*,*D*). The inhibitory effect of the deaf ear was more abundant, occurring in 78.1% of the recorded positions (significantly higher in comparison with the hearing ear effect, Wilcoxon–Mann–Whitney test, $p = 0.002$). The strength of the inhibitory effect of the deaf ear remained, however, in the range of control animals (HCs and CDCs, compare also to Fig. 7).

Taken together, we have found substantially reorganized excitatory–inhibitory interactions in both cortical hemispheres of uCDCs. The hearing ear showed a strengthened excitatory effect in binaural conditions, while the deaf ear exerted a mild inhibitory effect in both cortical hemispheres. Consequently, nearly all units receiving a crossed projection from a deaf ear could be excited by an uncrossed projection from a hearing ear, whereas a majority of the units receiving a crossed projection from a hearing ear could be inhibited by an uncrossed projection from a deaf ear. The present study thus provided evidence of the hearing ear preference in both cortical hemispheres in uCDCs.

Discussion

The presented results document a reorganized representation of ILDs by substituting the crossed-ear dominance with hearing ear dominance in both cortical hemispheres in uCDCs. Binaural interactions revealed enhanced excitatory and reduced inhibitory effect of the hearing ear, while the deaf ear showed weakened excitation and a preserved (and more frequent) inhibition of the responses to the overrepresented hearing ear in uCDCs (Fig. 8). These findings, together with near insensitivity to ITDs, support the aural preference syndrome (Gordon et al., 2015; Gordon and Kral, 2019). It explains the preference of the previously better-hearing ear in asymmetric hearing in children following bilateral CIs (Burdo et al., 2016; Myhrum et al., 2017; Sangen et al., 2019; Vanderauwera et al., 2020; Rauch et al., 2021).

Whereas ITD sensitivity is resolved at the level of the medial superior olivary complex (MSO) and is largely driven by binaural

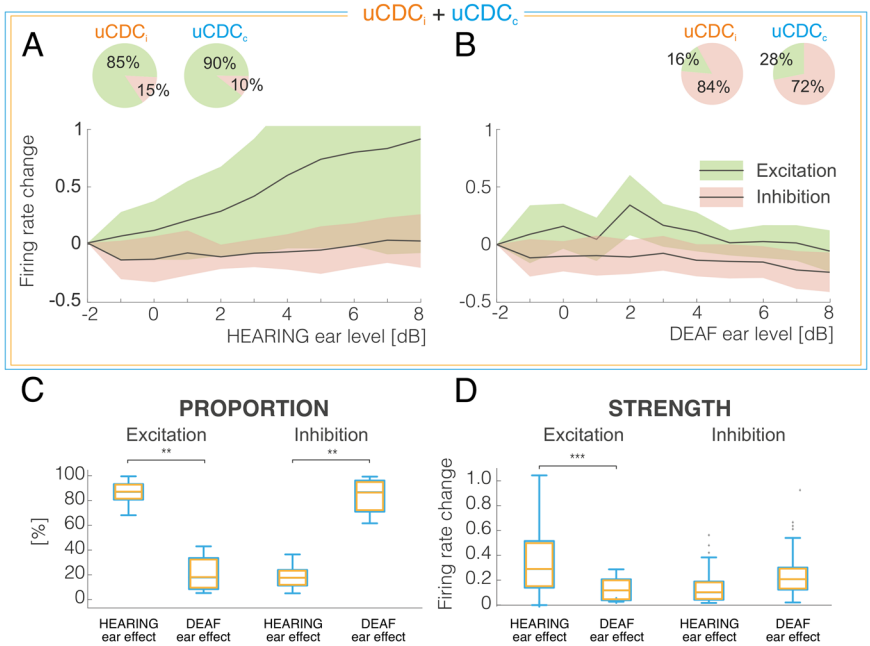

Figure 8. ILD responses under ABI variable condition in uCDCs. To evaluate the effect of the hearing condition of the ear on the responses, in addition to keeping the crossed ear at +6 dB and varying the uncrossed-ear stimulation, in a subset of 288 units, we further switched the ears and kept the uncrossed ear at +6 dB and varied the crossed ear. The results were sorted by varying ears (hearing or deaf). ***A***, The recording sites expressing overall excitatory and inhibitory binaural interactions are shown separately (means in black, standard deviations as pale red and pale green fillings) for the varying levels at the hearing ear. The pie charts show the relative numbers of the recording sites expressing excitation and inhibition in each cortical hemisphere, showing a similar preference for the excitatory (green) responses in both hemispheres. ***B***, Same as in ***A*** for varying levels at the deaf ear. Excitatory responses are weaker and less frequent when varying the deaf ear level (green). Inhibitory responses have a similar magnitude as in ***A*** but were more abundant in both hemispheres (red). ***C***, Statistical comparison of the proportion of cortical positions with excitatory (left) and inhibitory (right) binaural interactions, demonstrating that excitation was more frequent with the hearing ear variable condition, but inhibition was more frequent in the deaf ear variable condition. Kruskal–Wallis test with Tukey–Kramer post hoc significance difference criterion, $**\sim p < 0.01$. ***D***, Same comparison for the extent of the firing rate change (strength of the excitatory and inhibitory effect). While the excitatory influence of the hearing ear was much stronger than the excitatory influence of the deaf ear, the ears did not differ in the extent of the inhibitory effect. Kruskal–Wallis test with Tukey–Kramer post hoc significance difference criterion, $***\sim p < 0.001$.

excitatory coincidence (modulated by inhibition), ILD sensitivity is resolved at the level of the lateral superior olive (LSO) and is largely caused by the inhibitory influence of one ear on the response of the other ear (Grothe et al., 2010). Previous studies analyzed mainly ITD processing in deafness and CI stimulation (Smith and Delgutte, 2007; Hancock et al., 2010, 2013; Tillein et al., 2010; Chung et al., 2019; Buck et al., 2021; Rosskothen-Kuhl et al., 2021). The effects on ILDs were studied using mild reversible hearing loss (Popescu and Polley, 2010; Polley et al., 2013). They documented weakening of the responsiveness to the poorer hearing ear and disruption of ILD sensitivity. Since these latter studies have been performed using acoustic stimulation on a species with limited ITD sensitivity, direct comparisons of representation of ITD and ILD cues were not possible in small mammals.

ITD processing has been previously analyzed in uCDCs, documenting a reduced ITD modulation depth in uCDCs compared with CDCs and HCs (Tillein et al., 2016). The direct comparison of ILD to ITD sensitivity in the present study demonstrated a differential effect of SSD on these cues. Such a dissociation provides the animal with constantly discrepant spatial information after binaural hearing restoration: flatter ITD responses document reduced positional information, while ILD responses correspond to a source ipsilateral to the hearing ear. No binaural cue thus reveals the true source location. Constantly discrepant incorrect binaural spatial information is one reason for spatial cue reweighting toward monaural cues in SSD (Keating and King, 2013).

Acoustic envelope ITD sensitivity was observed in the LSO (Finlayson and Caspary, 1991). In the present study, ITD processing was unlikely relying on the LSO only: (1) there was a dissociation of the effects of SSD on ITD and ILD sensitivity; (2) the mean best ITDs with CIs in HCs were similar to acoustic stimulation (Smith and Delgutte, 2007; Tillein et al., 2010); and (3) the peak-type and biphasic-type ITD sensitivity functions that are abundantly observed in cats with CI stimulation (Smith and Delgutte, 2007; Hancock et al., 2010; Tillein et al., 2010) are unlikely to be the sole consequence of LSO processing.

There was a remarkable hemisphere-specific reorganization of excitatory–inhibitory interactions in uCDCs. In the cortical hemisphere ipsilateral to the hearing ear, increasing stimulation strength of the uncrossed (hearing) ear leads to excessive excitatory interactions and downregulated inhibitory interactions. This effect was found in ∼80% of the responding positions, and also the strength of the interaction was significantly shifted in favor of excitation. Similar changes with respect to the hearing ear have been observed following cochlear ablation [inferior colliculus (IC), Kitzes et al., 1995; McAlpine et al., 1997; Vale and Sanes, 2002; Vale et al., 2004; the primary auditory cortex, Reale et al., 1987; McMullen et al., 1988]. On the other hand, increasing the uncrossed stimulation from the deaf ear yielded a predominantly inhibitory interaction at both hemispheres, in strength similar to HCs and CDCs (Figs. 6–8). This finding has not been reported before, since stimulation at the deaf ear has not been possible following cochlear ablation.

The overall effect of the deaf ear on the hearing ear response involved a less frequent and weaker excitatory and more frequent (but not enhanced) inhibitory interaction (Fig. 8*C*,*D*). The proportion of such inhibitory interactions was higher and covered the majority of units in both hemispheres, thus representing a

complementary phenomenon to the general excitatory effect of the hearing ear. Consequently, the deaf ear exerted a weak inhibitory or neutral influence in both cortices, resulting in the virtual absence of binaural facilitation (cf. Tillein et al., 2016). Nevertheless, the deaf ear alone was able to evoke reliable although weak responses on both hemispheres.

The weak influence of the deaf ear on the binaural response together with strong hearing ear preference in both cortical hemispheres (Fig. 8) implies a functional disconnection of the two ears in acutely implanted SSDs. On the other hand, the auditory system has the potential for at least partial integration in the course of time in implanted SSD and sequentially implanted children (Illg et al., 2013, 2019; Polonenko et al., 2017; Anderson et al., 2022; Arras et al., 2022).

Many studies observed adaptive modifications in subcortical auditory structures in developmental asymmetric hearing (Nordeen et al., 1983; Kitzes and Semple, 1985; Saada et al., 1996; McAlpine et al., 1997; Kotak and Sanes, 2000; Vale and Sanes, 2000; Vale et al., 2004; Hutson et al., 2008; O'Neil et al., 2010; Xiong et al., 2013). The present results are most likely a consequence of such subcortical reorganizations. The results in uCDCs are explicable by brainstem adaptations involving homeostatic and spike timing–dependent plasticity (Froemke, 2015; Field et al., 2020; McFarlan et al., 2022):

1. A homeostatic increase in sensitivity of the ipsilateral and contralateral MSO, with neurons eventually mainly driven by the hearing ear and less by the deaf ear (for corresponding morphology difference in HCs and CDCs, see Tirko and Ryugo, 2012). This may cause a saturation response to the previously hearing ear and the near absence of response modulation by ITD.
2. Changes in the ipsilateral inferior colliculus (IC) leading to a predominantly excitatory effect of the hearing ear in the ipsilateral hemisphere:
   (a) In uCDCs, the ipsilateral IC always receives coincident excitation (from ipsilateral MSO) and inhibition (from ipsilateral LSO). Noncoincident excitation from the contralateral LSO and cochlear nucleus is absent due to deafness of the contralateral ear. Consequently, all postsynaptic activity is tightly paired with inhibitory input. Early in development, a similar condition induces long-term depression of inhibitory synapses (LSO, Kotak and Sanes, 2000; IC, Vale and Sanes, 2000; auditory cortex, Vickers et al., 2018). The consequence is a weakened inhibition (from ipsilateral LSO to ipsilateral IC). Loss of inhibition following cochlear ablation has been documented in the IC ipsilateral to the hearing ear (Vale and Sanes, 2002; Vale et al., 2004; Hutson et al., 2008), together with an increase in IC responsiveness to the hearing ear (Nordeen et al., 1983; Kitzes and Semple, 1985; McAlpine et al., 1997).
   (b) Loss of inhibition in the ipsilateral IC would allow potentiation of remaining excitatory synapses and strengthen the input from the ipsilateral MSO and contralateral IC (Xiong et al., 2013).
3. A depression of the inhibitory synapse would not take place in the contralateral LSO due to silencing of postsynaptic activity by strong inhibition from the hearing ear (and no excitation from the deaf ear) in uCDCs. However, the contralateral LSO would be strongly active during the brief developmental period before inhibition attains a hyperpolarizing effect.
4. After reactivating the deaf ear, the outputs of contralateral LSO are candidates for conveying its inhibitory influence in the contralateral IC. The effect can be transmitted to the other hemisphere (1) by the commissure of Probst (Aitkin and Phillips, 1984) that in unilateral cochlear ablation weakens its inhibitory component (Vale et al., 2004) and (2) the projection from the contralateral IC to the ipsilateral MGB (Andersen et al., 1980). Additionally, the deaf ear inhibits the ipsilateral LSO, conveying less binaural excitation to the contralateral IC.
5. Due to inactivity in the deaf auditory nerve, the projections to and from the contralateral cochlear nucleus may be preserved but weakened (Saada et al., 1996; O'Neil et al., 2010), explaining the weaker responses to the monaural stimulation of the deaf ear compared with the hearing ear (Tillein et al., 2016).

This sequence of events, partly hypothetical, is consistent with findings on cochlear ablation and SSD and relies only on mechanisms previously described. It encourages direct studies in the brainstem.

In conclusion, the cortical representation of ITD and ILD cues becomes inconsistent following single-sided deafness: while ITDs become uninformative, the ILDs are always in favor of the hearing ear. The presented neuronal reorganizations are in line with predominant responses to the previously hearing ear, consistent with the aural preference syndrome (Kral et al., 2013a,b; Gordon et al., 2015; Gordon and Kral, 2019). When comparing the effect of the ears in uCDCs, the neural mechanisms involve a strong excitation from the previously hearing ear and a weak excitation and similarly strong (but more abundant) inhibition from the previously deaf ear.

References

Aitkin LM, Phillips SC (1984) The interconnections of the inferior colliculi through their commissure. J Comp Neurol 228:210–216.

Andersen RA, Roth GL, Aitkin LM, Merzenich MM (1980) The efferent projections of the central nucleus and the pericentral nucleus of the inferior colliculus in the cat. J Comp Neurol 194:649–662.

Anderson CA, Cushing SL, Papsin BC, Gordon KA (2022) Cortical imbalance following delayed restoration of bilateral hearing in deaf adolescents. Hum Brain Mapp 43:3662–3679.

Arras T, Boudewyns A, Swinnen F, Zarowski A, Philips B, Desloovere C, Wouters J, Van Wieringen A (2022) Longitudinal auditory data of children with prelingual single-sided deafness managed with early cochlear implantation. Sci Rep 12:9376.

Buck AN, Rosskothen-Kuhl N, Schnupp JW (2021) Sensitivity to interaural time differences in the inferior colliculus of cochlear implanted rats with or without hearing experience. Hear Res 408:108305.

Burdo S, Giuliani A, Dalla Costa L (2016) Active inhibition of the first over the second ear implanted sequentially. Eur Ann Otorhinolaryngol Head Neck Dis 133:S31–S35.

Chase SM, Young ED (2007) First-spike latency information in single neurons increases when referenced to population onset. Proc Natl Acad Sci U S A 104:5175–5180.

Chung Y, Buechel BD, Sunwoo W, Wagner JD, Delgutte B (2019) Neural ITD sensitivity and temporal coding with cochlear implants in an animal model of early-onset deafness. J Assoc Res Otolaryngol 20:37–56.

Field RE, D'amour JA, Tremblay R, Miehl C, Rudy B, Gjorgjieva J, Froemke RC (2020) Heterosynaptic plasticity determines the set point for cortical excitatory-inhibitory balance. Neuron 106:842–854.e4.

Finlayson PG, Caspary DM (1991) Low-frequency neurons in the lateral superior olive exhibit phase-sensitive binaural inhibition. J Neurophysiol 65:598–605.

Froemke RC (2015) Plasticity of cortical excitatory-inhibitory balance. Annu Rev Neurosci 38:195–219.
Gordon K, Henkin Y, Kral A (2015) Asymmetric hearing during development: the aural preference syndrome and treatment options. Pediatrics 136:141–153.
Gordon K, Kral A (2019) Animal and human studies on developmental monaural hearing loss. Hear Res 380:60–74.
Gordon KA, Wong DDE, Papsin BC (2013) Bilateral input protects the cortex from unilaterally-driven reorganization in children who are deaf. Brain 136:1609–1625.
Grothe B, Pecka M, McAlpine D (2010) Mechanisms of sound localization in mammals. Physiol Rev 90:983–1012.
Hancock KE, Chung Y, Delgutte B (2013) Congenital and prolonged adult-onset deafness cause distinct degradations in neural ITD coding with bilateral cochlear implants. J Assoc Res Otolaryngol 14:393–411.
Hancock KE, Noel V, Ryugo DK, Delgutte B (2010) Neural coding of interaural time differences with bilateral cochlear implants: effects of congenital deafness. J Neurosci 30:14068–14079.
Hartmann R, Topp G, Klinke R (1984) Discharge patterns of cat primary auditory fibers with electrical stimulation of the cochlea. Hear Res 13: 47–62.
Heid S, Hartmann R, Klinke R (1998) A model for prelingual deafness, the congenitally deaf white cat–population statistics and degenerative changes. Hear Res 115:101–112.
Hutson KA, Durham D, Imig T, Tucci DL (2008) Consequences of unilateral hearing loss: cortical adjustment to unilateral deprivation. Hear Res 237: 19–31.
Illg A, Giourgas A, Kral A, Büchner A, Lesinski-Schiedat A, Lenarz T (2013) Speech comprehension in children and adolescents after sequential bilateral cochlear implantation with long interimplant interval. Otol Neurotol 34:682–689.
Illg A, Sandner C, Büchner A, Lenarz T, Kral A, Lesinski-Schiedat A (2019) The optimal inter-implant interval in pediatric sequential bilateral implantation. Hear Res 372:80–87.
Keating P, King AJ (2013) Developmental plasticity of spatial hearing following asymmetric hearing loss: context-dependent cue integration and its clinical implications. Front Syst Neurosci 7:123.
Kitzes LM, Kageyama GH, Semple MN, Kil J (1995) Development of ectopic projections from the ventral cochlear nucleus to the superior olivary complex induced by neonatal ablation of the contralateral cochlea. J Comp Neurol 353:341–363.
Kitzes LM, Semple MN (1985) Single-unit responses in the inferior colliculus: effects of neonatal unilateral cochlear ablation. J Neurophysiol 53:1483–1500.
Klinke R, Kral A, Heid S, Tillein J, Hartmann R (1999) Recruitment of the auditory cortex in congenitally deaf cats by long-term cochlear electrostimulation. Science 285:1729–1733.
Kotak VC, Sanes DH (2000) Long-lasting inhibitory synaptic depression is age- and calcium-dependent. J Neurosci 20:5820–5826.
Kral A, Dorman MF, Wilson BS (2019) Neuronal development of hearing and language: cochlear implants and critical periods. Annu Rev Neurosci 42: 47–65.
Kral A, Heid S, Hubka P, Tillein J (2013a) Unilateral hearing during development: hemispheric specificity in plastic reorganizations. Front Syst Neurosci 7:93.
Kral A, Hubka P, Heid S, Tillein J (2013b) Single-sided deafness leads to unilateral aural preference within an early sensitive period. Brain 136:180–193.
Kral A, Lomber SG (2015) Deaf white cats. Curr Biol 25:R351–R353.
Kral A, Tillein J, Hartmann R, Klinke R (1999) Monitoring of anaesthesia in neurophysiological experiments. Neuroreport 10:781–787.
Kral A, Tillein J, Hubka P, Schiemann D, Heid S, Hartmann R, Engel AK (2009) Spatiotemporal patterns of cortical activity with bilateral cochlear implants in congenital deafness. J Neurosci 29:811–827.
McAlpine D, Martin RL, Mossop JE, Moore DR (1997) Response properties of neurons in the inferior colliculus of the monaurally deafened ferret to acoustic stimulation of the intact ear. J Neurophysiol 78:767–779.
McFarlan AR, Chou CYC, Watanabe A, Cherepacha N, Haddad M, Owens H, Sjöström PJ (2022) The plasticitome of cortical interneurons. Nat Rev Neurosci 24:80–97.
McMullen NT, Goldberger B, Suter CM, Glaser EM (1988) Neonatal deafening alters nonpyramidal dendrite orientation in auditory cortex: a computer microscope study in the rabbit. J Comp Neurol 267:92–106.
Middlebrooks JC, Clock AE, Xu L, Green DM (1994) A panoramic code for sound location by cortical neurons. Science 264:842–844.
Middlebrooks JC, Green DM (1991) Sound localization by human listeners. Annu Rev Psychol 42:135–159.
Myhrum M, Strøm-Roum H, Heldahl MG, Rødvik AK, Eksveen B, Landsvik B, Rasmussen K, Tvete OE (2017) Sequential bilateral cochlear implantation in children: outcome of the second implant and long-term use. Ear Hear 38:301–313.
Nordeen KW, Killackey HP, Kitzes LM (1983) Ascending projections to the inferior colliculus following unilateral cochlear ablation in the neonatal gerbil, Meriones unguiculatus. J Comp Neurol 214:144–153.
O'Neil JN, Limb CJ, Baker CA, Ryugo DK (2010) Bilateral effects of unilateral cochlear implantation in congenitally deaf cats. J Comp Neurol 518:2382–2404.
Polley DB, Thompson JH, Guo W (2013) Brief hearing loss disrupts binaural integration during two early critical periods of auditory cortex development. Nat Commun 4:2547.
Polonenko MJ, Gordon KA, Cushing SL, Papsin BC (2017) Cortical organization restored by cochlear implantation in young children with single sided deafness. Sci Rep 7:16900.
Polonenko MJ, Papsin BC, Gordon KA (2018) Limiting asymmetric hearing improves benefits of bilateral hearing in children using cochlear implants. Sci Rep 8:13201.
Popescu MV, Polley DB (2010) Monaural deprivation disrupts development of binaural selectivity in auditory midbrain and cortex. Neuron 65:718–731.
Quiroga RQ, Nadasdy Z, Ben-Shaul Y (2004) Unsupervised spike detection and sorting with wavelets and superparamagnetic clustering. Neural Comput 16:1661–1687.
Rauch AK, Arndt S, Aschendorff A, Beck R, Speck I, Ketterer MC, Jakob TF, Hassepass F (2021) Long-term results of cochlear implantation in children with congenital single-sided deafness. Eur Arch Otorhinolaryngol 278:3245–3255.
Reale RA, Brugge JF, Chan JC (1987) Maps of auditory cortex in cats reared after unilateral cochlear ablation in the neonatal period. Brain Res 431: 281–290.
Rosskothen-Kuhl N, Buck AN, Li K, Schnupp JWH (2021) Microsecond interaural time difference discrimination restored by cochlear implants after neonatal deafness. Elife 10:e59300.
Ryugo DK, Kretzmer EA, Niparko JK (2005) Restoration of auditory nerve synapses in cats by cochlear implants. Science 310:1490–1492.
Ryugo DK, Rosenbaum BT, Kim PJ, Niparko JK, Saada AA (1998) Single unit recordings in the auditory nerve of congenitally deaf white cats: morphological correlates in the cochlea and cochlear nucleus. J Comp Neurol 397: 532–548.
Saada AA, Niparko JK, Ryugo DK (1996) Morphological changes in the cochlear nucleus of congenitally deaf white cats. Brain Res 736:315–328.
Sangen A, Dierckx A, Boudewyns A, Dhooge I, Offeciers E, Wouters J, Desloovere C, van Wieringen A (2019) Longitudinal linguistic outcomes of toddlers with congenital single-sided deafness—six with and twelve without cochlear implant and nineteen normal hearing peers. Clin Otolaryngol 44:671–676.
Smith ZM, Delgutte B (2007) Sensitivity to interaural time differences in the inferior colliculus with bilateral cochlear implants. J Neurosci 27:6740–6750.
Tillein J, Hubka P, Kral A (2016) Monaural congenital deafness affects aural dominance and degrades binaural processing. Cereb Cortex 26:1762–1777.
Tillein J, Hubka P, Syed E, Hartmann R, Engel AK, Kral A (2010) Cortical representation of interaural time difference in congenital deafness. Cereb Cortex 20:492–506.
Tirko NN, Ryugo DK (2012) Synaptic plasticity in the medial superior olive of hearing, deaf, and cochlear-implanted cats. J Comp Neurol 520:2202–2217.
Vale C, Juiz JM, Moore DR, Sanes DH (2004) Unilateral cochlear ablation produces greater loss of inhibition in the contralateral inferior colliculus. Eur J Neurosci 20:2133–2140.
Vale C, Sanes DH (2000) Afferent regulation of inhibitory synaptic transmission in the developing auditory midbrain. J Neurosci 20:1912–1921.
Vale C, Sanes DH (2002) The effect of bilateral deafness on excitatory and inhibitory synaptic strength in the inferior colliculus. Eur J Neurosci 16: 2394–2404.

Vanderauwera J, Hellemans E, Verhaert N (2020) Research insights on neural effects of auditory deprivation and restoration in unilateral hearing loss: a systematic review. J Clin Med 9:812.

Vickers ED, Clark C, Osypenko D, Fratzl A, Kochubey O, Bettler B, Schneggenburger R (2018) Parvalbumin-interneuron output synapses show spike-timing-dependent plasticity that contributes to auditory map remodeling. Neuron 99:720–735.e6.

Xiong XR, Liang F, Li H, Mesik L, Zhang KK, Polley DB, Tao HW, Xiao Z, Zhang LI (2013) Interaural level difference-dependent gain control and synaptic scaling underlying binaural computation. Neuron 79:738–753.